FINAL REPORT

Title:	**Novel Transparent Phosphor Conversion Matrix with High Thermal Conductivity for Next Generation Phosphor-Converted LED-based Solid State Lighting**
Proposal Number:	DE-EE0006702
Prime Organization:	Carnegie Mellon University Materials Science & Engineering Pittsburgh, PA 15213
Technical Point of Contact:	Professor Michael Bockstaller Department of Materials Science & Engineering Wean Hall 4307 Carnegie Mellon University 5000 Forbes Avenue, Pittsburgh, PA 15213-3890 Tel: 412-268-2709 | Fax: 412-268-7596 Email: bockstal@andrew.cmu.edu
Administrative Point of Contact:	Ms. Rochelle Athey, CRA Associate Vice Provost for Sponsored Programs Carnegie Mellon University 5000 Forbes Avenue, WQED Building Pittsburgh, PA 15213 Tel 412-268-8746 | Fax: 412-268-6279 Email: osp-preaward@andrew.cmu.edu
OSRAM Sylvania POC	Adam Scotch OSRAM SYLVANIA 71 Cherry Hill Drive, Danvers, MA 01915 Phone: 9787501734 | Fax: 9787502152
Period of Performance:	August 15, 2014-October 30, 2016

TABLE OF CONTENTS

I. Executive Summary

The low thermal conductivity of state-of-the-art polymer encapsulants ($k \sim 0.15$ $Wm^{-1}K^{-1}$) limits the efficiency and power density of current phosphor conversion light emitting diodes (pc-LEDs). The technical objective of this project was to demonstrate synthesis and processing schemes for the fabrication of polymer hybrid encapsulants with a thermal conductivity exceeding $k = 0.4$ $Wm^{-1}K^{-1}$ for LED applications. The 'hybrid polymer' approach encompasses the dispersion of high thermal conductivity particle fillers (zinc oxide, ZnO as well as the alpha-polymorph of alumina, Al_2O_3) within a polysiloxane matrix (poly(dimethylsiloxane), PDMS as well as poly(phenyl methyl siloxane), PPMS) to increase the thermal conductivity while maintaining optical transparency and photothermal stability at levels consistent with LED applications. To accomplish this goal, a novel synthesis method for the fabrication of nanosized ZnO particles was developed and a novel surface chemistry was established to modify the surface of zinc oxide particle fillers and thus to enable their dispersion in poly(dimethyl siloxane) (PDMS) matrix polymers. Molecular dynamics and Mie simulations were used to optimize ligand structure and to enable the concurrent mixing of particles in PDMS/PPMS embedding media while also minimizing the thermal boundary resistance as well as optical scattering of particle fillers. Using this approach the synthesis of PDMS/ZnO hybrid encapsulants exhibiting a thermal conductivity of 0.64 $Wm^{-1}K^{-1}$ and optical transparency > 0.7 mm^{-1} was demonstrated. A forming process based on micromolding was developed to demonstrate the forming of particle filled PDMS into film and lens shapes. Photothermal stability testing revealed stability of the materials for approximately 4000 min when exposed to blue light LED (450 nm, 30 W/cm^2).

One postgraduate and seven graduate students were supported by the project. The research performed within this project led to fifteen publications in peer-reviewed journals and one patent application. The grant stimulated a multi-investigator research collaborations among seven investigators at Carnegie Mellon University to address the challenge of encapsulants in pc-LED applications. The grant also catalyzed the future collaboration between researchers at Carnegie Mellon University and OSRAM Sylvania to address challenges associated with the use if polymers in LED applications.

II. Project Goals and Accomplishments

2.1 Project Goal

The overall goal of this effort was to demonstrate the synthesis and processing of novel polymer hybrid encapsulants with a thermal conductivity exceeding 0.4 $Wm^{-1}K^{-1}$ for LED applications. To accomplish this goal the effort was organized into five thrust areas that focused on: (i) synthesis and structural characterization; (ii) modeling and characterization of thermal transport properties; (iii) modeling and characterization of optical properties; (iv) processing; and (v) fabrication, integration and performance evaluation. For each thrust two tasks and eight milestones (*i.e.* four milestones for each task) were defined to guide the research within year 1 and year 2 of the performance period.

2.2 Comparison of Proposed Project Goals and Project Accomplishments

In the following, the different task areas and milestones for each thrust are summarized along with a description of actual project accomplishments. Where appropriate deviations from the original plan are highlighted and a description of the motivation and impact of the deviation from the original project plan is provided.

2.2.1 Thrust 1: Material Synthesis

Year 1 The Recipient shall investigate synthesis of PMMA and Styrene acrylonitrile (SAN)-tethered Al_2O_3 and ZnO particles by surface-initiated atom transfer radical polymerization (SI-ATRP). The Recipient shall confirm the successful synthesis of these materials by electron microscopy, thermal gravimetric analysis (TGA), X-ray diffraction, size-exclusion chromatography, and other analytical methods. The Recipient shall evaluate the purified particles by TGA to confirm the presence of the polymer. The Recipient shall use size exclusion chromatography to confirm the absence of non-tethered polymeric chains. The Recipient shall establish the absence of aggregates by dynamic light scattering.

Year 2 The Recipient shall develop and apply a procedure to uniformly disperse and covalently link the polymeric tethered particle fillers to the siloxane matrix to make hybrid encapsulant materials with inorganic fraction in the range 5-40% by volume. First, polymer-tethered particle systems shall be end-functionalized with vinyl functionalities using, for example, nucleophilic substitution of bromine moieties, for the subsequent crosslinking within the siloxane resin. Second, polymer-tethered particles shall be dispersed in siloxane intermediates (ϕ_{inorg} = 1-30 vol%). Vinyl functionality shall be optionally converted to silicon hydride (SiH) functionality by hydrosilation with an excess of M^HM^H. The dispersion of particles within siloxane intermediates shall be evaluated using dynamic light scattering. In the case that unforeseen challenges in the dispersion of particle fillers should occur, lower molecular weight intermediates (x = 7) shall be applied. After dispersion, polymer tethered particle fillers with vinyl termini shall be crosslinked with $M^HD_x^{Ph}M^H$ polymers by hydrosilation. Alternatively, vinyl terminated particles shall be crosslinked with $M^{Vi}D_x^{Ph}M^{Vi}$ intermediates and commercially available SiH functional materials, such as $M^HD_x^{Ph2}M^H$ (x = 1 or 2.5) and resins of type $M_4^HT_6^{Ph}$, $M_6^HT_4^{Ph}$. The final microstructure of hybrid encapsulants shall be determined using a combination of electron and atom probe imaging, small-angle X-ray scattering as well as spectroscopic techniques.

Milestone Definition

Milestone Year1.1 - Demonstrate synthesis of 1g PMMA@Al_2O_3 with *N* in range 10-100 and grafting density in the range of σ = 0.1-0.7 nm^{-2} (M3)
Milestone Year1.2 – Demonstrate synthesis of 1 g PSAN@Al_2O_3 with *N* in range 10-100 and grafting density in the range of σ = 0.1-0.7 nm^{-2} (M6)
Milestone Year1.3 - Demonstrate synthesis of PMMA@ZnO with *N* in range 10-100 and grafting density in the range of σ = 0.1-0.7 nm^{-2} (M9)
Milestone Year1.4 - Demonstrate synthesis of PSAN@ZnO with *N* in range 10-100 and grafting density in the range of σ = 0.1-0.7 nm^{-2} (M12)
Milestone Year2.1 - Demonstrate functionalization of PMMA@Al_2O_3 /PMMA@ZnO using chemical analysis (M15)
Milestone Year2.2 - Demonstrate synthesis of 1g siloxane/PMMA@Al_2O_3, siloxane/PMMA@ZnO encapsulant with inorganic fraction in the range f = 0.05-0.4 (M18)
Milestone Year2.3 - Demonstrate functionalization of PSAN@Al_2O_3 /PSAN@ZnO using chemical analysis (M21)
Milestone Year2.4 - Demonstrate synthesis of 1g siloxane/PSAN@Al_2O_3, siloxane/PSAN@ZnO encapsulant with inorganic fraction in the range f = 0.05-0.4 (M24)

Summary Accomplishment
All milestones have been accomplished.

A novel process for the surface modification of alpha-alumina nanoparticles was developed. The process was shown to enable dense grafting of polymeric ligands. (*ACS Appl. Mat. & Interfaces* **2016**, *8*, 5458-5465).
A novel process for the synthesis of nanometer sized zinc oxide particles was developed. A new process for the surface modification of nanometer-sized zinc oxide particles was developed. The new process was shown to enable the dense grafting of polymer ligands. (*Langmuir*, **2016**, *32*, 13207–13213).
A novel process for the dispersion of nanoparticles into polymer resins was developed. The novel process was shown to significantly enhance the loading fraction of inorganic fillers and enable the synthesis of high refractive index polymer glasses (*ACS Appl. Mat. & Interfaces, accepted*).
A novel process for the dispersion of ligand modified ZnO particles into PDMS resins resulting in thermal conductivity of 0.64 $Wm^{-1}K^{-1}$ was developed (*International Patent Application PCT/US17/14723*).

Note: During months 1-3 of performance period 2 difficulties in fabricating homogeneous mixtures of polymer-modified Al_2O_3 and ZnO nanoparticles within PDMS became apparent. The aggregation of particles resulted in the embrittlement of hybrid PDMS encapsulants as well as pronounced scattering losses that reduced the photothermal stability of PDMS hybrid films. To counter this challenge, a novel ligand chemistry was developed on the basis of octylamine to enable the uniform dispersion of ZnO particles in PDMS matrix. The resulting particles showed uniform dispersion up to inorganic contents of 20 vol%.

2.2.2 Thrust 2: Modeling and Characterization of Thermal Transport Properties of Polymer-Tethered Particle Fillers

Year 1 Atomistic modeling tools (i.e. molecular dynamics (MD) simulations and density functional theory (DFT) calculations) shall be applied to determine the governing parameters for thermal boundary resistance of polymer-tethered interfaces. "Direct methods" (i.e. a heat flow applied across the interface to calculate the resulting temperature drop) as well as DFT shall be utilized to predict the role of interfacial bonding strength and length of polymer tethers on thermal transport in hybrid encapsulant systems.

Year 2 Thermal conductivity measurements of hybrid thin films shall be performed using a high fidelity pump-probe laser technique called Frequency Domain Thermoreflectance (FDTR). Siloxane-based hybrid films shall be deposited on Si substrates and coated with an evaporated Au film (~50 nm thick) for FDTR measurements. An intensity modulated pump laser (λ_{Pump} = 488nm) shall periodically heat the sample surface and a probe laser (λ_{Probe} = 532nm) shall monitor the resultant thermal wave via thermoreflectance. The measured amplitude and phase lag of the probed surface temperature (relative to the pumped heat flux) shall be fit to a multi-layer heat conduction model to determine the thermal properties of the sample.

Milestone Definition

Milestone Year1.1 - Establish framework for modeling of atomic interactions (M3)
Milestone Year1.2 - Establish effect of bond strength on thermal conductivity. Demonstrate calculation of thermal boundary resistance for different bond strength approximations (in the range 50-200 kJ/mol) using computer simulation (M6)
Milestone Year1.3 - Establish equilibrium conformation of polymer tether (M9)
Milestone Year1.4 - Establish effect of chain length on thermal conductivity. Demonstrate calculation of thermal transport properties of polymer graft layers with a thickness corresponding to a chain length *N* in the range N = 10 – 100 using computer simulation (M12)
Milestone Year2.1 - Demonstrate FDTR and/or heat flow measurements on siloxane with better than 20 % reproducibility (M15)
Milestone Year2.2 - Demonstrate FDTR and/or heat flow measurements on siloxane/PMMA@Al_2O_3 composites. Establish thermal conductivity for composites with inorganic fraction within the range f = 0.05 – 0.4 (M18)
Milestone Year2.3 - Demonstrate FDTR and/or heat flow measurements on siloxane/PMMA@ZnO. Establish thermal conductivity for composites with inorganic fraction within the range f = 0.05 – 0.4 (M21)
Milestone Year2.4 - Demonstrate FDTR and/or heat flow measurements on PSAN hybrids with inorganic fraction within the range f = 0.05 – 0.4. Establish material compositions with $k >= 1$ W/mK (M24)

Summary Accomplishment
Milestones have been partially accomplished. A thermal conductivity of 0.64 $Wm^{-1}K^{-1}$ was demonstrated.

Molecular dynamics simulations were performed to elucidate the effect of molecular structure and bonding strength of organic ligands on the thermal conductivity of polymer/particle interfaces. It was demonstrated that dense tethering of aliphatic ligands result in the alignments of ligands normal to the surface thus enhancing phonon transport across the particle/matrix interface (*Nature Commun*. **2015**, *6*, 1-8).
The thermal conductivity of polymer/particle composites was evaluated using FDTR as well as heat flow measurements. The thermal conductivity was shown to increase with increasing ligand density and bonding strength, in agreement with theoretical predictions (*Polymer* **2016**, *93*, 72-77).
The thermal conductivity of PDMS/ZnO hybrid encapsulants was evaluated using heat flow measurements. A thermal conductivity of $k = 0.64$ $Wm^{-1}K^{-1}$ was demonstrated for composites with an inorganic filling fraction of zinc oxide of 5% by volume (*International Patent Application PCT/US17/14723*).

2.2.3 Thrust 3: Modeling and Characterization of Optical Properties of Polymer-Tethered Particle Fillers and Composites Thereof

Year 1 The effect of polymer-graft modification on the optical properties of ZnO and Al_2O_3 particles embedded in siloxane shall be evaluated using the effective medium theory. Numerical simulations using core-shell Mie models shall be used to evaluate the limitations of effective medium theory and to evaluate the effect of polymer tethering on the scattering properties of alumina particles ($d \sim 30$ nm). The Recipient shall conduct the optical modeling to gain an understanding of the effect of hybrid encapsulants on the transparency of DCMS material systems consisting of ternary blends of graded-interface particle/siloxane/phosphor. The Recipient shall use finite element simulations to test the hypothesis that, in the limit of small particle additives, the scattering of phosphor inclusions within the DCMS can be reduced in the presence of graded-interface particle fillers by reduction of the scattering contrast between phosphor and encapsulant.

Year 2 The Recipient shall conduct optical characterization of the hybrid encapsulant materials by acquiring extinction spectra using a UV-VIS spectrometer. As losses due to both absorption and scattering will likely occur, separation of these contributions shall be achieved by measuring the true absorption via collection of all scattered light.

Milestone Definition

Milestone Year1.1 - Demonstrate effective medium calculation to predict optical properties of polymer-tethered particles corresponding to synthetic system (M3)
Milestone Year1.2 - Demonstrate Mie calculation for core-shell particle systems corresponding to synthetic system (M6)
Milestone Year1.3 - Demonstrate calculation/prediction of PMMA@ZnO configuration allowing for a total reduction of the scattering cross section of PMMA@ZnO/siloxane/phosphor composite systems by 50% assuming $d_{ZnO} = 20$ nm, filling fraction ZnO = 0.05-0.4, $d_{phosphor} = 5$ mm, filling fraction phosphor = 0.4 using the effective medium model (M9)

Milestone Year1.4 - Demonstrate calculation/prediction of PMMA@ZnO configuration allowing for a total reduction of the scattering cross section of PMMA@ZnO/siloxane/phosphor composite systems by 50% assuming d_{ZnO} = 20 nm, filling fraction ZnO = 0.05-0.3, $d_{phosphor}$ = 5 mm, filling fraction phosphor = 0.4 using (core-shell) Mie theory (M12)
Milestone Year2.1 - Determine optical absorption and transparency of siloxane (M15)
Milestone Year2.2 - Determine extinction cross section of siloxane/PMMA@Al_2O_3 with inorganic fraction in the range f = 0.05 – 0.4 (M18)
Milestone Year2.3 - Determine extinction cross section of siloxane/PMMA@ZnO with inorganic fraction in the range f = 0.05 – 0.4 (M21)
Milestone Year2.4 - Determine extinction cross section of PSAN hybrids with inorganic fraction in the range f = 0.05 – 0.4. Identify materials with transparency equal to or better than 0.7/mm (M24)

Summary Accomplishment
All milestones have been accomplished.

A core shell Mie model was developed to simulate the effect of polymer graft modification on the optical transmittance of polymer nanocomposites. The model was applied to determine polymer graft compositions that minimize scattering losses in polymer hybrids. The results were validated against experimental transmittance determined from UV/vis spectrophotometry. (*Langmuir* **2015**, *30*, 14434-14442).

The optical properties of hybrid encapsulants were evaluated using UV/vis. Transparencies > 0.7 mm^{-1} were demonstrated.

2.2.4 Thrust 4: Forming and Processing of Encapsulant Matrix as well as PDMS Hybrid Encapsulants

Year 1 The Recipient shall focus on establishing spin-cast and micromolding conditions to facilitate the processing of siloxane intermediates that form the basis of current encapsulant materials. A design-of-experiments (DoE) study shall be conducted through fractional factorial design by varying spinning conditions, viscosity, flow rate, pressure and polymer-melt temperature. The average thickness and uniformity, characterized by surface roughness and form errors, shall be used as the performance metric. A multivariate analysis of variance (ANOVA) study shall be conducted to identify the statistically significant process parameters. The Recipient shall measure the uniformity using white-light interferometry.

Year 2 Mechanical characteristics of siloxane-intermediates/particle dispersions and cross-linked hybrid encapsulants shall be determined using rheological for liquid dispersions and dynamical mechanical analysis (DMA) for solid hybrids. The mechanical property characteristics shall determine the processing conditions, using a micro-molding test-bed with precise loading, motion, and heating capabilities, including sensors to measure temperature distributions, ram loads, and displacements for the shaping of hybrid encapsulants into dome and lens form factors. Shape analysis using electron and optical imaging shall be used to indicate process capability in terms of feature size, shape, edge sharpness, undercut, and aspect ratio. Repeatability of the

process shall also be determined. A DoE analysis shall be used, and an ANOVA shall be conducted to determine the main and compounded effects of different parameters on geometric accuracy, and shape (e.g., edge sharpness, area). Forming conditions shall be evaluated as a function of molecular architecture, composition and inorganic content as well as crosslink ratio of the encapsulant.

Milestone Definition

Milestone Year1.1 - Demonstrate measurement of mechanical properties of siloxane intermediates (M3)
Milestone Year1.2 - Demonstrate siloxane lens shape with diameter in the range 3-10 mm (M6)
Milestone Year1.3 - Complete DoE analysis (M9)
Milestone Year1.4 - Complete ANOVA. Demonstrate experimental conditions allowing for reproducible fabrication of siloxane lens shapes with surface roughness below 200 nm and variability of roughness of less than 20% in batch-to-batch process (M12)
Milestone Year2.1 - Demonstrate microforming of lens shaped siloxane specimen with diameter in the range of 3-5 mm (M15)
Milestone Year2.2 - Establish rheological and mechanical properties of hybrids (M18)
Milestone Year2.3 - Demonstrate microforming of siloxane/PMMA@ZnO and siloxane/PMMA@Al_2O_3 into lens shape with diameter in the range 3 – 5 mm (M21)
Milestone Year2.4 - Demonstrate microforming of PSAN hybrids into lens shape with diameter in the range 3 – 5 mm (M24)

Summary Accomplishment
Milestones have been partially accomplished.

Processing of PDMS intermediates into film and lens shapes with surface roughness less than 200 nm and batch-to-batch variability of surface roughness of less than 20% were demonstrated using spin casting and micromolding.
Processing of PDMS hybrid materials into lens forms with surface roughness less than 200 nm and batch-to-batch variability of surface roughness of less than 20% were demonstrated using spin casting and micromolding. The forming processed was demonstrated to be amenable to the forming of a wide range of polymer hybrid compositions (*Soft Matter* **2016**, *12*, 3527-3537).
The mechanical properties of PDMS/ZnO hybrid materials were determined using dynamic mechanical analysis as well as tensile testing.

Nature, motivation and implication of deviations from original plan: During months 1-3 of performance period 2 difficulties in fabricating homogeneous mixtures of polymer-modified Al_2O_3 and ZnO nanoparticles within PDMS became apparent. Aggregation of particles resulted in the embrittlement of hybrid PDMS encapsulants. Embrittlement caused mechanical failure (i.e. fracture) of films during processing. To resolve this challenge a novel ligand chemistry was developed to enable the dispersion of particles within PDMS and to avoid embrittlement (see explanation of Thrust 1 in section 2.2.1). This, however, took nine months to accomplish. To avoid delays caused by the synthesis of uniform PDMS hybrids, reference PDMS/silica hybrid materials (provided by Dow Corning) were used instead to establish process parameters for the forming of PDMS hybrids.

2.2.5 Thrust 5: Forming and Processing of Encapsulant Matrix as well as PDMS Hybrid Encapsulants

Year 1 As a typical LED is expected to last >10,000 hours at 35 A/cm^2, rapid life testing shall be designed to test if these materials could withstand 10,000 hours of operation without material degradation and change in optical properties. The appropriate metric to describe the photo-thermal degradation shall be developed for rapid testing, and implemented in order to meet the industry requirements.

Year 2 Hybrid encapsulant/phosphor DCMS shall be fabricated using standard techniques. Analysis of thermal transport characteristics shall be performed using steady-state heat flow analysis. The effect of polymer-tethered ZnO/Al_2O_3 particles on the transparency of DCMS compositions shall be evaluated using UV/vis spectrophotometry. The effect of polymer-tethered ZnO/Al_2O_3 particles on the luminescence, down-conversion efficiency, and light extraction characteristics of phosphors shall be determined using spectroscopic and photometric methods configured for such studies.

Milestone Definition

Milestone Year1.1 - Determination of rate of transmission loss as function of light intensity (in range 0.1 – 1 W/cm^2) and temperature (in the range T = 25 – 150 °C)) of pristine polymers PSAN, PMMA (M3)
Milestone Year1.2 - Determination of rate of transmission loss as function of light intensity (in range 0.1 – 1 W/cm^2) and temperature (in the range T = 25 – 150 °C)) of PMMA@Al_2O_3 (M6)
Milestone Year1.3 - Determination of rate of transmission loss as function of light intensity (in range 0.1 – 1 W/cm^2) and temperature (in the range T = 25 – 150 °C)) of PSAN@Al_2O_3 (M9)
Milestone Year1.4 - Determination of rate of transmission loss as function of light intensity (in range 0.1 – 1 W/cm^2) and temperature (in the range T = 25 – 150 °C)) of PMMA@ZnO (M12)
Milestone Year2.1 - Determination of rate of transmission loss as function of light intensity (in range 0.1 – 1 W/cm^2) and temperature (in the range T = 25 – 150 °C)) of PSAN@ZnO (M15)
Milestone Year2.2 - Determination of rate of transmission loss as function of light intensity (in range 0.1 – 1 W/cm^2) and temperature (in the range T = 25 – 150 °C)) of siloxane/PMMA@Al_2O_3 and DCMS system. Determine QE at 35 A/cm^2 (M18)
Milestone Year2.3 - Determine QE of siloxane/PMMA@ZnO and siloxane/PMMA@Al_2O_3 at 35 A/cm^2 (M21)
Milestone Year2.4 - Determine QE of PSAN hybrid encapsulant DCMS at 35 A/cm^2. Demonstrate QE >= 95% at 35 A/cm^2 (M24)

Summary Accomplishment
Milestones have been partially accomplished.

An in-house heatflow meter was constructed to enable the measurement of thermal conductivity of polymer hybrid films under conditions equivalent to LED applications. The heat flow meter was applied to determine the thermal conductivity of hybrid siloxanes and to demonstrate a maximum thermal conductivity of k = 0.64 +/- 0.03 Wm^{-1}K^{-1} of films prepared within this project.

A photothermal stability tester was developed to assess the stability of hybrid siloxanes under LED type operation conditions (i.e. irradiation of films at 450 nm LED operating at 35 mA/cm^2 at film temperature of 150 degree Celsius). The stability of films was determined by measurement of transmittance losses at T = 150 degree Celsius to 'simulate' accelerated degradation of films.

Nature, motivation and implication of deviations from original plan: During months 1-3 of performance period 2 difficulties in fabricating homogeneous mixtures of polymer-modified Al_2O_3 and ZnO nanoparticles within PDMS became apparent. Aggregation of particles within the PDMS matrix causes scattering and thermal losses that result in the rapid degradation of films under testing conditions. It was determined that priority should be given to the assessment of photothermal stability to promote the development of film compositions with photothermal stability characteristics consistent with LED application. For reasons of practicality the integration of hybrid PDMS in LED chip sets was omitted. The novel ligand chemistry based on octylamine (developed in the last quarter of performance period 2) was found to enable PDMS/ZnO hybrids with significantly increased photothermal stability.

III. Research Activities

In the following, the technical details pertaining to the major research efforts performed within the scope of the project "Novel Transparent Phosphor Conversion Matrix with High Thermal Conductivity for Next Generation Phosphor-Converted LED-based Solid State Lighting" will be discussed. The emphasis will be on respective research objectives: (i) synthesis of particle fillers and their inclusion in PDMS matrices, (ii) a core-shell Mie model to predict the scattering losses in PDMS hybrids, (iii) the processing of hybrid encapsulants into film lens shapes and (iv) the evaluation of the photothermal stability of PDMS hybrids.

3.1 Synthesis of ligand tethered Al_2O_3 particles and PDMS composites thereof

3.1.1 Activation and surface modification of alpha alumina particles.

Alpha-alumina (α-Al_2O_3) was chosen as the preferred polymorph for the synthesis of high thermal conductivity composite materials due to its high intrinsic thermal conductivity of $k = 42$ $Wm^{-1}K^{-1}$. Synthesis of PDMS/ α-Al_2O_3 hybrids involves three different steps: (i) the surface activation of / α-Al_2O_3; (ii) the tethering of polymeric ligands to the surface of particles and (iii) the subsequent embedding of ligand modified particles into PDMS matrix. Of these three steps, the first step is original and has not been reported in the literature. Rather, it has been reported in the literature that the alpha polymorph is not accessible to surface modification. Alumina starting materials were tested from several vendors (Sigma, US Nano, and others, the process was found to work for all batch samples that were obtained. The details of the surface modification are presented below. The process has also been published in the international patent application *PCT/US17/14723* as well as *Appl. Mat. & Interfaces* **2016**, *8*, 5458-5465.

Activation is accomplished by exposure of particles samples to strong alkali or acidic conditions as shown in Figure 1.

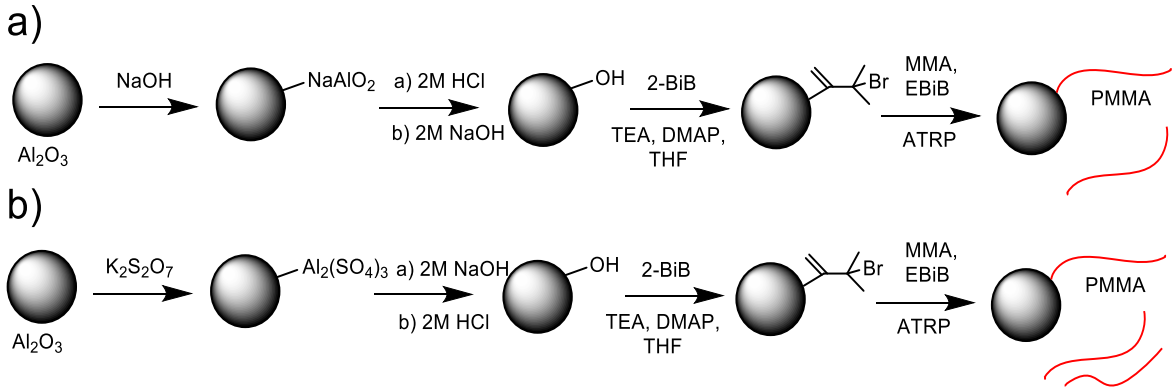

Figure 1. Illustration of surface treatment and subsequent polymer modification of alpha-alumina nanoparticles.

PMMA and PSAN brushes were grafted from the activated alumina surface using surface-initiated atom transfer radical polymerization. The samples were characterized by GPC and TGA as shown in Figure 2.

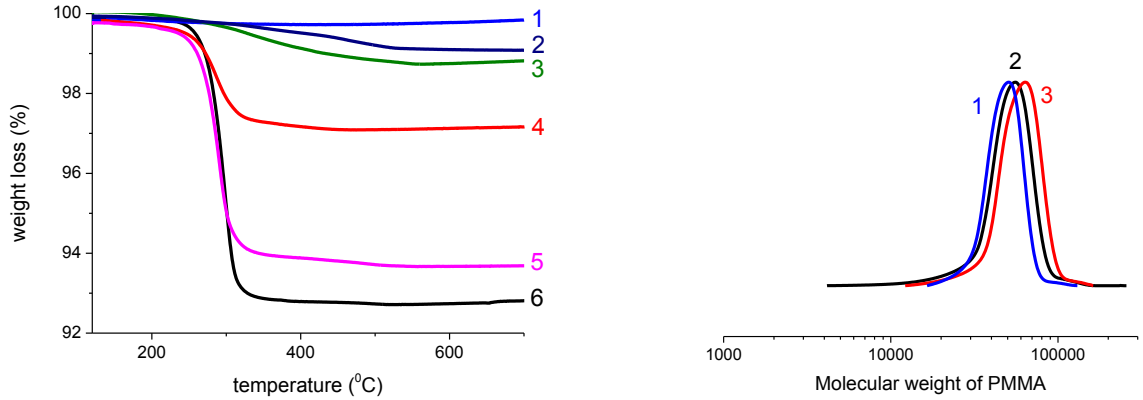

Figure 2. Left: representative TGA curves of pristine α alumina nanoparticles (1), initiator-modified alumina nanoparticles, activated in molten $K_2S_2O_7$ (2), initiator-modified alumina nanoparticles, activated in molten NaOH (3), PMMA-modified alumina without any activation (4), PMMA-modified alumina activated in molten NaOH for 15 min (5), PMMA-modified alumina activated in molten $K_2S_2O_7$ for 15 min (6). Right: GPC traces of free polymer initiated by sacrificial initiator in solution concurrently with polymer grafted from the surface of alumina nanoparticles with no surface activation (blue), alumina nanoparticles activated in molten NaOH for 15 min (black), and alumina nanoparticles activated in molten $K_2S_2O_7$ for 15 min (red).

Figure 3 below shows the dependence of the achievable grafting density on the method of surface activation (as determined by TGA and SEC analysis).

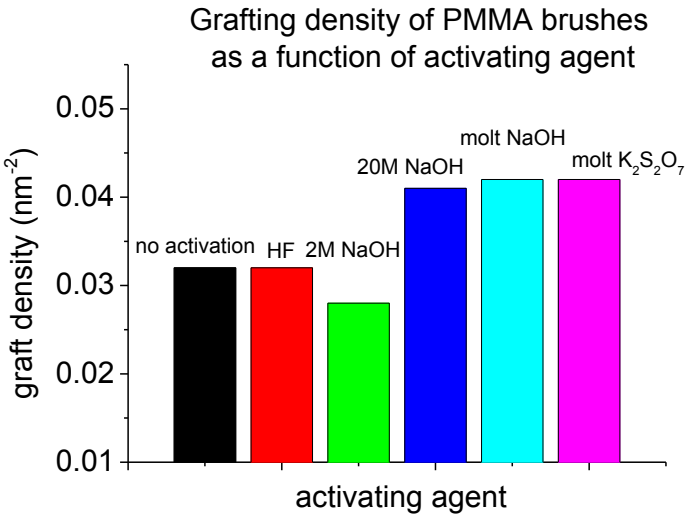

Figure 3. Grafting density of PMMA brushes on α alumina surface as a function of surface activation by various agents. Activation with molten NaOH and molten $K_2S_2O_7$ was carried out for 15 min, activation with other agents was carried out for 12 h. Reaction conditions: $[Al_2O_3$-Br]/[EBiB]/[MMA]/[$CuCl_2$]/[CuCl]/[PMDETA] = 1/1/1000/0.3/1/2 in anisole (50 vol%), DMF (2 vol%). T = 60 °C.

Figure 4 depicts the dependence of the maximum achievable grafting density on the time of exposure to activating conditions.

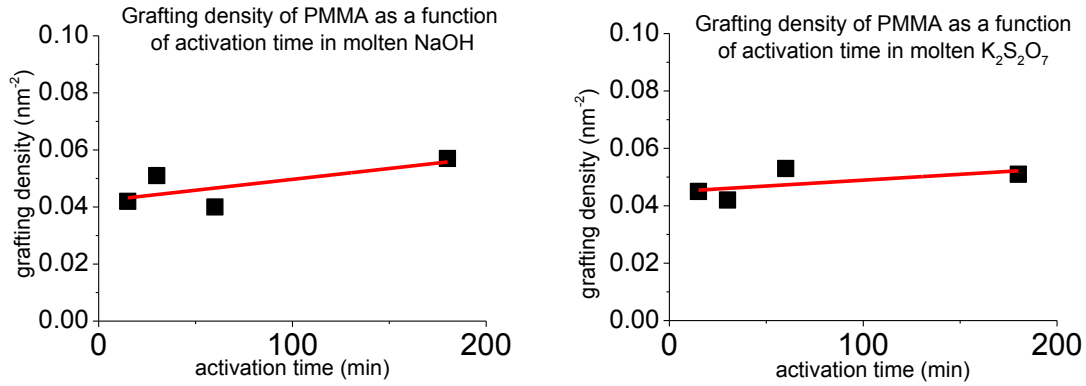

Figure 4. Grafting density of PMMA brushes on the surface of α alumina as a function of activation time in molten NaOH (left) and $K_2S_2O_7$ (right). The linear fit trend line is shown in red. Reaction conditions: $[Al_2O_3\text{-Br}]/[EBiB]/[MMA]/[CuCl_2]/[CuCl]/[PMDETA]$ = 1/1/1000/0.3/1/2 in anisole (50 vol%), DMF (2 vol%). T = 60 °C. Reaction time 3 h.

The effect of polymer graft modification is illustrated by comparing of the dispersion stability of alumina particle solutions. While pristine particles were found to flocculate after only minutes, suspensions of polymer tethered analogs were found to be stable for up to 24 h. The increased dispersion stability provides major benefits for the fabrication of PDMS/alumina hybrids. The comparison of dispersions is shown in Figure 5.

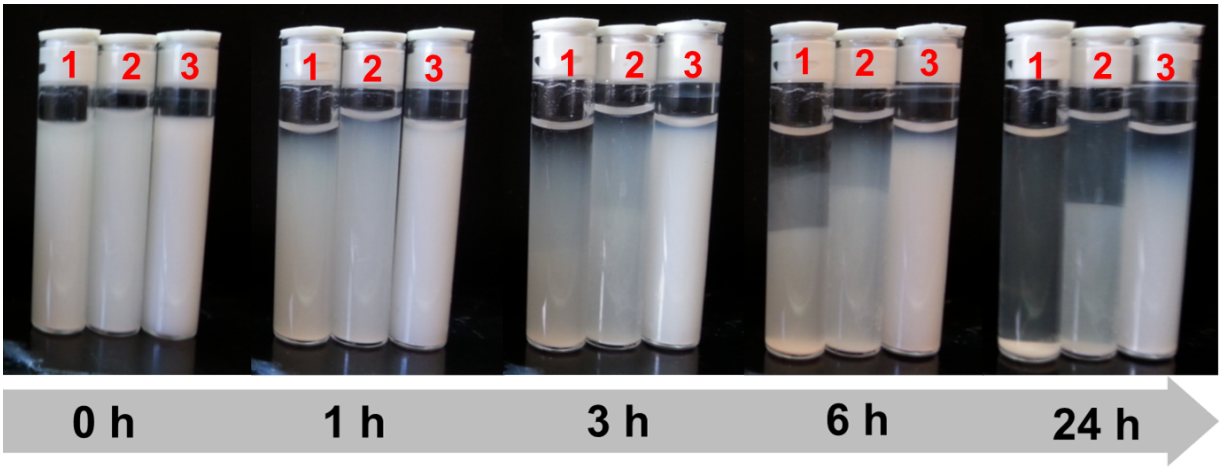

Figure 5. Stability of alumina particles dispersed in THF as a function of time. **1**: pristine α alumina particles, **2**: PMMA-modified non-activated alumina particles, **3**:PMMA-modified alumina particles, activated in molten NaOH for 60 min.

3.1.2 Fabrication of PDMS/alumina hybrids

Commercial LED PDMS encapsulant resin (OE-6630) was obtained from Dow (Justin Bolt). It has 2 parts, A – containing vinyl groups and catalys, B containing hydrosilane groups. The optimal mixture ratio is 1A:4B by weight. The structure of OE-6630 is unknown. As a second material system vinyl-siloxane and hydrosilane chemicals with known structures were obtained from Gelest. The latter were used exclusively for the preparation of PDMS/ZnO hybrids. Figure 6 illustrated the reaction mechanism as proposed on the basis of the structure provided by Gelest.

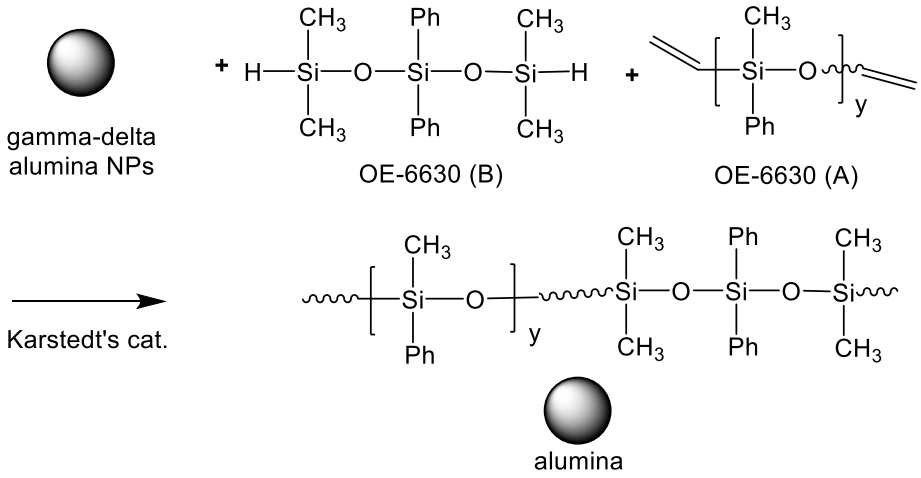

Figure 6. Proposed reaction scheme for PDMS hybrid material synthesis.

A representative procedure was as follows:
1. Dispersing inorganic particles (alumina, ZnO or silica) in THF in sonicator bath for 60 min. Typically, 0.5 g of particles is dispersed in 2-3 ml of THF in a closed vial.
2. Addition of OE-6630 B component to the dispersion, followed by 30 sec vortexing.
3. Addition of OE-6630 A component (catalyst carrier), followed by 30 sec vortexing.
4. Transfering the mixture into circular Teflon mold, 25 or 35 mm in diameter, sealed with a Teflon film at the bottom.
5. Evaporation of THF within 4-12 h in open air at room T, or evaporation of THF at 70 C for 1 h.
6. Placing the mold with mixture to the oven preheated to 120 C for 4 – 12 h.
7. Removing the cured film from the mold.

Films were characterized using TGA and electron imaging. Figure 7 depicts representative micrographs of a sample of PDMS/alumina (10 wt%).

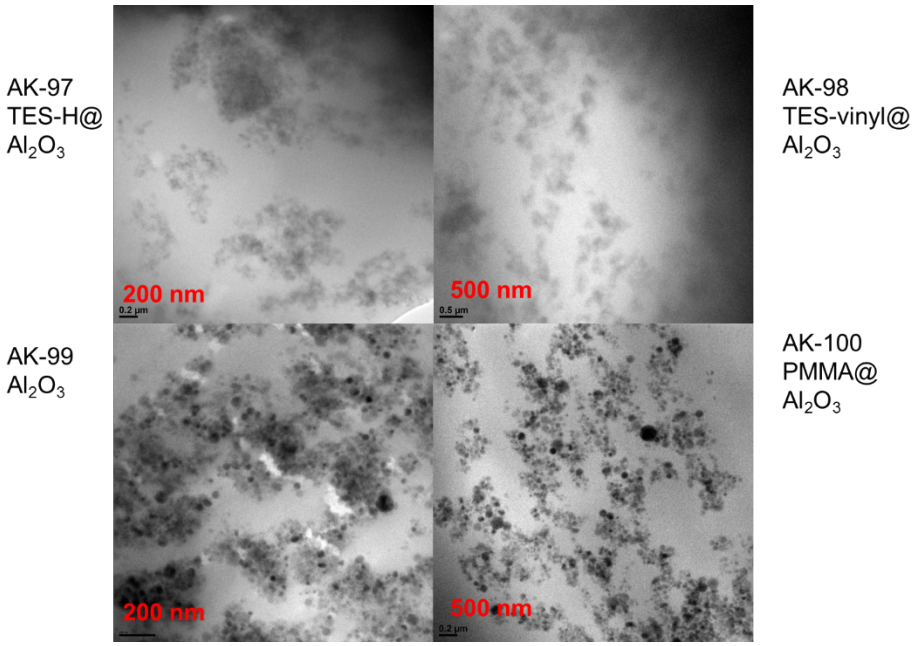

Figure 7. TEM images depicting microstructure of PMMA-alumina dispered in PDMS. Significant agglomeration of particle fillers is observed.

In agreement with electron imaging the PDMS composite films did show significant scattering losses (see Figure 8).

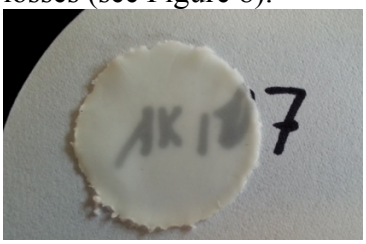

Figure 8. Picture of PDMS/PMMA-alumina composite film (film thickness = 0.3 mm). Particle aggregation results in significant scattering losses.

Conclusion on PDMS/Alumina hybrid materials.

A novel method for the synthesis of polymer modified alumina particle fillers was established. The process involves the activation of the surface of particles and results in significantly higher (~ten-fold) grafting densities as previously known methods. However, while the process is found to significantly prolonged dispersion stabilities, particles were found to be immiscible in PDMS matrix. This is interpreted as a consequence of insufficient grafting and resulting surface matrix interactions that favor agglomeration of particle fillers. The resulting hybrid materials exhibited significant scattering losses and are not appropriate for LED application. It was concluded that *alumina particle fillers are not a viable platform for the synthesis of hybrid encapsulants for LED applications*.

3.2 Synthesis of ligand tethered ZnO particles and PDMS composites thereof

3.2.1 Synthesis of polymer grafted ZnO nanoparticles by "grafting-from" method

Functionalization of ZnO nanoparticles. Poly(methyl methacrylate) (PMMA) and poly(styrene-*co*-acrylonitrile) (PSAN) grafted ZnO nanoparticles were synthesized in two steps. In the first step, initiator functionalized ZnO (ZnO-Br) nanoparticles were synthesized by the following procedure: 25 mL of ZnO dispersion (10 g ZnO in butyl acetate) were dissolved in 200 mL of dry THF in a round bottom flask, and TEA (5.14 mL, 37 mmol) was then added to the solution. The flask was sealed, transferred to an ice bath and stirred. 2-BiB (4.56 mL, 37 mmol) was then slowly added, drop by drop, to the solution. The flask then was stirred for another 48 h at room temperature. The product was washed 3 times with cold methanol and dried in air for 24 h. After removal of all solvent, ZnO-Br NPs were obtained.

Synthesis of PMMA or PSAN was subsequently performed using activators generated by electron transfer (AGET) ATRP from ZnO-Br. The polymer brushes were grafted from the surface of initiator-modified zinc oxide nanoparticles as follows: 1.0 g ZnO-Br nanoparticles, Me_6TREN (0.038 g, 0.143 mmol), 30 M solution of $CuBr_2$ in DMF (1 mL, 0.030 mmol), anisole (10 mL), MMA (10 mL, 95 mmol) or St (10.5 mL, 95 mmol) and AN (3.7 mL, 57 mmol) were placed in 50 mL Schlenk flask equipped with a magnetic stir bar. The flask was sealed, and the resulting solution was bubbled with N_2 for 30 minutes. 15 mM of a solution of $Sn(EH)_2$ in anisole (1 mL, 0.015 mmol) was added to the flask to reduce $CuBr_2$. The flask was then immersed to an oil bath set at 70 ºC, and the reaction mixture was kept under these conditions for the desired time, MMA system for 1 h, and the SAN system for 24 h. The reaction mixture was exposed to air to stop the reaction. Products were precipitated by addition of the solution to cold methanol. The samples were then centrifuged, and the products were redissolved in THF, the resulted solution was cloudy and unstable. The samples were then centrifuged again to remove the insoluble impurities, which were non-functionalized pristine ZnO nanoparticles. The resulted solutions then were concentrated and precipitated into methanol. Solid products were dried in air for the further characterizations.

Particle systems were characterized using DLS, TEM and TGA analysis, respectively. Particles were found to agglomerate and were not found to form stable dispersions in THF or PDMS precursor polymers.

3.2.2 Synthesis of polymer grafted ZnO nanoparticles by "grafting-to" method

In the grafting-to method polymers are pre-synthesized and subsequently tethered to particle surfaces by means of a coupling reaction using proper end group functionalization. While grafting-to methods generally result in less well defined products (as compared to grafting-from, see 3.2.1) they are scalable and economically viable. Several grafting-to coupling reactions were explored during the course of the project. First, by using block copolymer tethers that exhibit a poly(acrylic acid) block which binds preferentially to the oxygen and hydroxyl groups on the ZnO surface. Second, by using amino-terminated polymers that form amidization reactions with hydroxyl groups on the ZnO surface. While both methods were expected to result in similar extent of polymer modification it was found that *only reaction with amine-functionlized ligands resulted in efficient exchange*. In the following a typical procedure for the grafting-to modification of ZnO particles using amine-terminated ligands will be presented.

3.2.3 Synthesis of PSAN capped ZnO by ligand exchange method

The ZnO nanoparticles were synthesized as reported previously. $Zn(EH)_2$ (45 g, 100.8 mmol) was mixed with DPE (80 mL) and OA (90 mL, 503.97 mmol) in a 250 mL three-neck flask equipped with a condenser and a thermometer. The stirred reaction mixture was heated to 175 ºC under a N_2 atmosphere. The temperature was held at 175 ºC for 45 minutes before heating the mixture to 230 ºC for another 60 minutes. After cooling to room temperature, the nanoparticles were isolated by precipitation in cold methanol. The resulting product was dispersed in THF to give a stock solution of 40 mg mL^{-1} for use in further experiments (Figure 9).

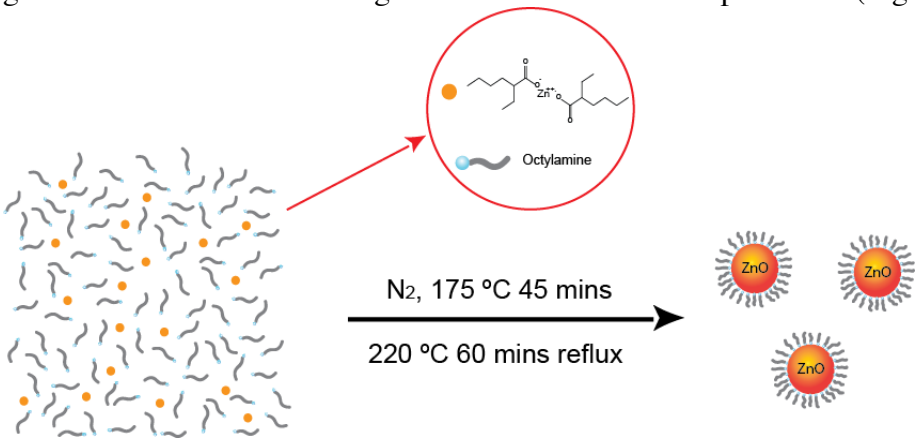

Figure 9. Illustration of synthesis of octyl amine OA capped ZnO NPs.

Synthesis of PSAN-NH_2 polymer ligand. The synthesis of PSAN-NH_2 polymer ligand included three steps: a) the synthesis of the ATRP initiator with a protected amino group, b) copolymerization of S and AN monomers by ARGET ATRP and c) deprotection of the amino group. The respective steps are outlined in Figure 10.

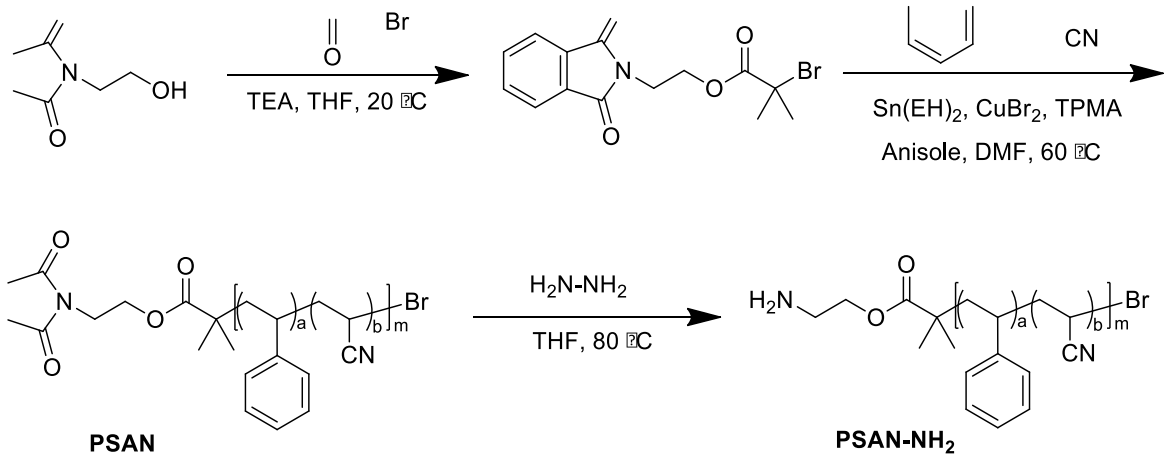

Figure 10. Synthesis scheme of PSAN-NH_2 polymer ligands.

a) NHP (16.3 g, 81.96 mmol) and TEA (14.28 mL, 102.45 mmol) were dissolved in 200 mL dry THF in a 500 mL round bottom flask fitted with a stirring bar, stirred in an ice bath. Then 2-BiBB (12.67 mL, 102.45 mmol) was added dropwise to the mixture over 30 minutes. After the

flask was stirred for another 24 h at room temperature, the reaction mixture was concentrated, and the residue was dissolved in 100 mL ethyl acetate. The solution was washed with a saturated aqueous $NaHCO_3$ solution (200 mL) twice and once with brine to remove the formed salt and byproducts. The final ATRP initiator was obtained by removing the ethyl acetate using rotary evaporation.

b) S (16 mL, 139.85 mmol), AN (5.5 mL, 83.91 mmol), Me_6TREN (0.075 mL, 0.28 mmol), anisole (7.2 mL), and 0.03 mol/L solution of $CuBr_2$ in DMF (0.5 mL, 0.015 mmol) were added to a dry 50 mL Schlenk flask. After the flask was sealed, the resulting solution was bubbled with N_2 for 30 minutes. Then, 300 mM of $Sn(EH)_2$ solution in anisole (1 mL, 0.30 mmol) was added to the flask to reduce a fraction of the $CuBr_2$. The flask was placed in an oil bath set at 60 ºC, and the reaction mixture was kept for the desired time. After the reaction mixture was exposed to air to stop the polymerization, the product was precipitated by addition of cold hexane, filtered and dried in air. The synthesis of the copolymers with different molecular weights was similar to the procedure described above, but with different targeted degrees of polymerization, as reported previously.

c) The obtained PSAN (8.3 g, 3.6 mmol, M_n=2300) was mixed with dry THF (150 mL) and hydrazine (1.08 mL, 34.5 mmol) in a 250 mL three-neck flask equipped with a condenser and a thermometer. The stirred reaction mixture was heated to 80 ºC under a N_2 atmosphere for 8 h. After cooling to room temperature, the insoluble byproduct was removed by centrifugation. The resulting solution was concentrated by rotary evaporation, and PSAN-NH_2 was isolated by precipitation in cold hexane and dried in air.

Synthesis of PSAN-capped ZnO nanoparticles. A general procedure for the ligand exchange reaction was as follows. A stock solution of OA-capped ZnO in THF (40 mg mL^{-1}, 25 mL) was mixed with DPE (30 mL) and PSAN-NH_2 (M_n = 1300, 1000 mg, 0.77 mmol) in a 100 mL two-neck flask equipped with a bubbler. The contents of the flask were bubbled with N_2. The stirred mixture was heated to 150 ºC under a N_2 atmosphere, and the temperature was maintained for 20 minutes to remove THF. Then the temperature was increased to 220 ºC for 2 h to facilitate removal of OA (b.p. = 175 ºC). The reaction mixture was cooled to room temperature and added to cold hexane to precipitate the product. After 1.0 g of resulting yellow powder was re-dissolved in 25 mL THF, the same volume of hexane was added to the solution, and the precipitate was isolated by centrifugation at 3000 g. Several "selective dissolution, precipitation, centrifugation," cycles were carried out to completely remove the free PSAN-NH_2 polymer ligands. The process is illustrated in Figure 11.

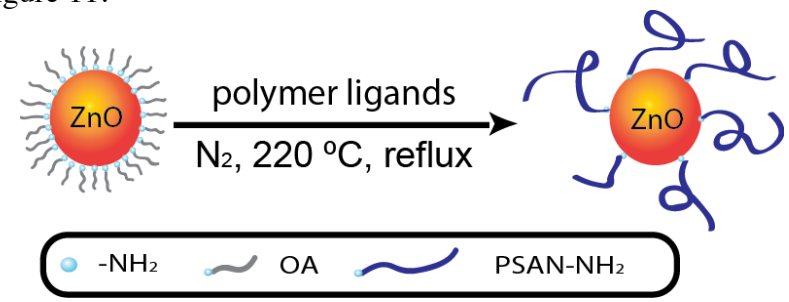

Figure 11. Synthesis scheme for PSAN capped ZnO.

Octylamine (OA) was chosen as ligand because of its appropriate boiling point of 175 ºC that prevents rapid evaporation during thermolysis of $Zn(EH)_2$. Figure 12a and 12b depict

representative electron micrographs (TEM) of OA-capped ZnO, revealing a uniform particle size with average diameter $\langle d \rangle = 5.23 \pm 0.61$ nm.

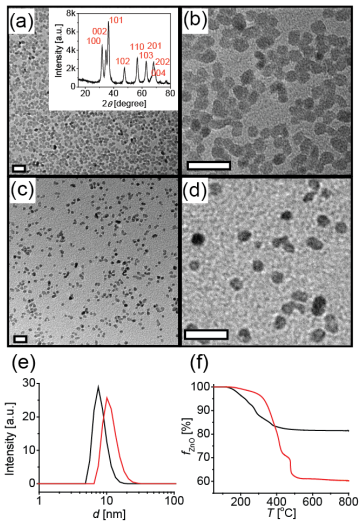

Figure 12. (a) and (b) TEM images of OA-capped 5 nm ZnO NPs, inset: XRD pattern of OA-capped ZnO; (c) and (d) TEM images of PSAN capped 5 nm ZnO NPs, M_n = 2300, M_w/M_n = 1.13; (e) Size distribution of OA/PSAN capped ZnO NPs measured by DLS in THF solution, intensity average particle size: OA-capped ZnO NPs, 7.5 nm, PSAN capped ZnO NP, 10.1 nm; (f) TGA traces of OA/PSAN capped ZnO NPs. Black line: OA-capped ZnO, red line: PSAN capped ZnO. Scale bars = 20 nm. Inset in Figure 12a depicts representative XRD pattern of OA-capped ZnO. Reflections correspond to the (100), (002), (101), (102) and (110) planes (PDF card nos: JCPDS-36-1451).

The typical particle yield of was 23%. X-ray diffraction analysis (see inset of Figure 12a) confirmed Wurtzite structure of ZnO. Dispersions of OA-capped ZnO NPs were stable in tetrahydrofuran (THF) or hexane for weeks, with negligible aggregation. Dynamic light scattering (DLS, Figure 12e) confirmed an intensity-average hydrodynamic size of about 7 nm in excellent agreement with TEM results. Thermogravimetric analysis revealed 83 wt% inorganic content (Figure 12f). From the inorganic content f_{ZnO} the ligand grafting density was determined to be 4.4 chains/nm^2.

Ligand exchange of OA with PSAN-NH_2 was performed in DPE at T = 180 ºC to concurrently drive the replacement reaction and extract unbound OA from the reaction mixture. The replacement reaction gave rise to a distinctive change in solubility characteristics. Whereas OA-capped ZnO NPs were stable in THF or hexane, PSAN-capped ZnO NPs after ligand exchange precipitated in hexane. Thus, free PSAN-NH_2 was removed by applying "selective precipitation, centrifugation, and dissolution" cycles. As shown in Figure 12e, the DLS confirmed the ligand replacement by revealing an increase of the hydrodynamic diameter from 7.5 to 10.1 nm. Electron micrographs of the final ZnO-PSAN product (Figure 12c and 12d) further revealed negligible aggregation of particles after ligand exchange. The purified PSAN capped ZnO NPs contain 60 wt% of ZnO (Figure 5f). Due to the large difference in steric hindrance, the grafting density of PSAN capped ZnO (0.7 chain/nm^2) was lower than OA-capped ZnO (4.4 chains/nm^2).

Conclusion Several new methods were introduced to facilitate the synthesis of polymer-modified alumina and zinc oxide particle systems. Table 1 lists the characteristics of all particle systems that were synthesized during the cause of the program.

Particle	Polymer/ Ligand	*N*	σ (nm^{-2})	ϕ_{inorg} (%)	approx. amount (mg)
Al_2O_3	PMMA	20-50	0.35	90	450
Al_2O_3	PMMA	350	NA	95	1000
Al_2O_3	PMMA	380	NA	93	1000
Al_2O_3	PMMA	NA	NA	34	500
Al_2O_3	PMMA	290	0.15	60	700
Al_2O_3	PSAN	230	0.01	92	700
Al_2O_3	PSAN	20-50	0.10	97	500
Al_2O_3	PSAN	16-24	0.50	92	500
Al_2O_3	PSAN	200	0.07	84	800
Al_2O_3	PSAN	8-32	0.25	91	500
ZnO	PMMA	2200	NA	15	500
ZnO	PMMA	137	0.06	92	200
ZnO	PMMA	1700	NA	36	1200
ZnO	PMMA	2000	NA	25	1400
ZnO	PSAN	25	NA	96	200
ZnO	PSAN	980	NA	44	600
ZnO	PSAN	400	0.10	96	200
ZnO	PSAN	1100	NA	29	350
ZnO	PDMS	15	0.4	NA	200
ZnO	OA	NA	1.2	83	2500
ZnO	HA	NA	1.25	89	1270
ZnO	BA	NA	NA	91	820

Table 1. *Subset of polymer-tethered particles synthesized to date. Alumina purchased from: 1.US – Nano (Stock #: US3008, US7010, http://www.us-nano.com/inc/sdetail/208, http://www.us-nano.com/inc/sdetail/623). 2. Nyacol (maxim has info). 3. Nanoarc (CAS No. 1344-28-1) (https://www.alfa.com/en/catalog/45586). Zinc Oxide purchased from: 1. US – Nano (Stock #: US3599, http://www.us-nano.com/inc/sdetail/7712). 2. Sigma Aldrich (CAS Number 1314-13-2, http://www.sigmaaldrich.com/catalog/ product/aldrich/721093?lang=en&region=US).*

Synthesis of PPMS capped ZnO by ligand exchange method α,ω-divinylpoly(methylphenylsiloxane) (PPMS) diamine were synthesized first (Figure 13). Then the same "ligand exchange" strategy was applied on OA capped ZnO NPs with PPMS diamine ligands. The resulted solutions were dialysized in THF for three cycles to remove free ligand and DPE solvent.

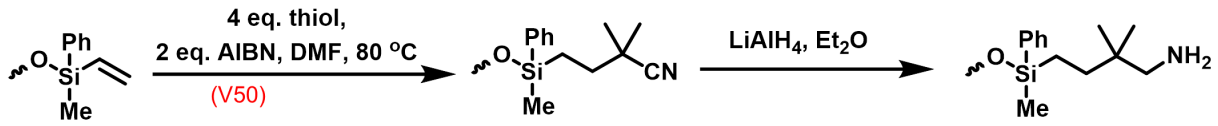

Figure 13. Synthesis of PPMS diamine.

A general procedure for the ligand exchange reaction was as follows. A stock solution of OA-capped ZnO in THF (40 mg mL^{-1}, 25 mL) was mixed with DPE (25 mL) and 1 g PPMS diamine in a 100 mL two-neck flask equipped with a bubbler. The contents of the flask were bubbled with N_2. The stirred mixture was heated to 150 ºC under a N_2 atmosphere, and the temperature was maintained for 20 minutes to remove THF. Then the temperature was increased to 220 ºC for 2 h to facilitate removal of OA (b.p. = 175 ºC). After the reaction, the solution was cooling down under atmosphere. DPE and free PPMS diamine ligands were removed by dialysis (THF) in 3 cycles.

3.2.4 Synthesis of PDMS/ZnO Hybrid Materials

Particles were dispersed in PPMS and PDMS resins following to the procedure outlined above. Both PMMA, PSAN, PDMS, PPMS and OA amine ligands were evaluated. The optical transmittance of composites was determined to assess the degree of particle dispersion (i.e. uniform dispersion is indicated by increased optical transparency). Octylamine (OA) ligands were found to be most effective in enabling particle dispersion.

In total, 66 composite formulations were evaluated during the course of the program. Best performance characteristics were found for PDMS/ZnO-OA hybrids as well as hexylamine (HA) analogs, for which a thermal conductivity of $k \sim 0.4$ $Wm^{-1}K^{-1}$ was determined and only small reduction of the optical transparency.

The optical properties of OA-ZnO, HA-ZnO and HA-ZnO/PDMS were studied using UV/vis spectrophotometry. Representative results are shown in Figure 14. As expected, the composite systems absorb light below 370 nm (corresponding to the band gap of ZnO) while materials are transparent at longer wavelengths. Interestingly the absorption edge of HA-ZnO/PDMS hybrids is slightly blue shifted compared to OA-ZnO/PDMS hybrids (not shown here). This is interpreted as a consequence of the smaller particle size in case of HA-ZnO ($<d>$ = 4 nm) as compared to OA/ZnO ($<d> \sim 6$ nm) and the increase of the band gap energy. It is currently not clear whether the decrease of particle size is ultimately favorable since the benefit of higher transparency might be outweighed by the larger specific surface area and the associated increase of thermal boundary resistance (future heat flow measurements will reveal optimum size). Current synthetic efforts focus on a systematic variation of synthesis conditions to enable the controlled variation of particle size

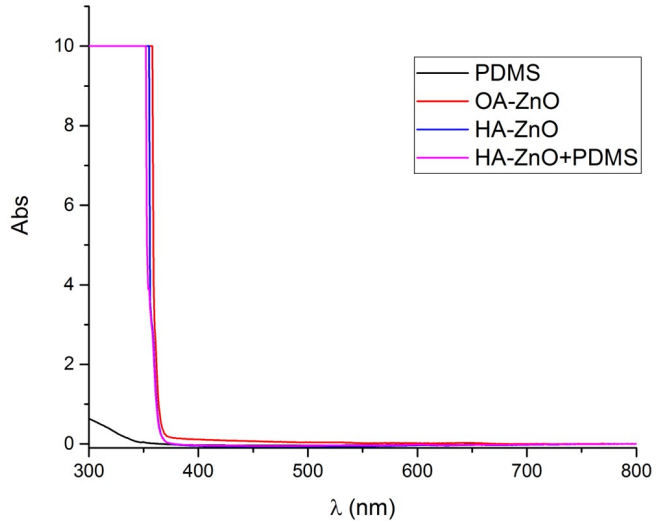

Figure 14. The UV-Vis absorption of PDMS, OA-ZnO, HA-ZnO and HA-ZnO PDMS mixture.

Figure 15 depicts a photograph of a HA-ZnO/PDMS film with inorganic content ϕ_{ZnO} ~ 55 wt% revealing the transparency of films. Crack formation is observed at the rim of the film and is indicative of embrittlement due to high particle content.

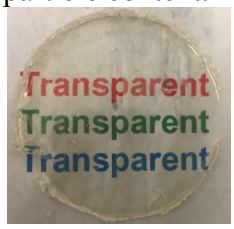

Figure 15. Picture of HA-ZnO/PDMS hybrid film with ϕ_{ZnO} ~ 55 wt%.

The cracking of films such as those shown in Figure 15 reveals a fundamental problem of PDMS hybrid materials, *i.e.* the fracture toughness of films decreases as the particle content increases. This is a common observation for cross-linked polymer hybrid materials and is related to particles acting as stress concentrators as well as barriers for microscopic plastic deformation during straining of the films. For LED applications this presents a twofold problem: first, it reduces the processibility of materials into desired form factors. Second, the low fracture toughness promotes cracking during the rapid volume expansion of the film during operation of the LED. The practical limitations of film processibility thus define a practical limit to the inorganic filling fraction.

To enhance processibility and crack resistance a new dispersion strategy was evaluated that we coin 'ternary hybrid approach'. In this approach a dense packing of large particle fillers (size ~ 120 nm) that are near index-matched to the PDMS embedding medium are used to 'partition space'. The surface chemistry of large particle fillers is engineered such that strong binding is accomplished to the PDMS matrix (this can be accomplished by choosing silica or siloxane-based large particle fillers). The filling fraction of large particles is chosen such that under conditions of volume shrinkage (during sample cross linking) a random close packed structures forms. ZnO particles are segregated to interstitial regions where dense particle networks are

being formed. This method has the advantage that dense networks of high thermal conductivity particle fillers form at rather low filling fraction of ZnO. Figure 16 illustrates the concept.

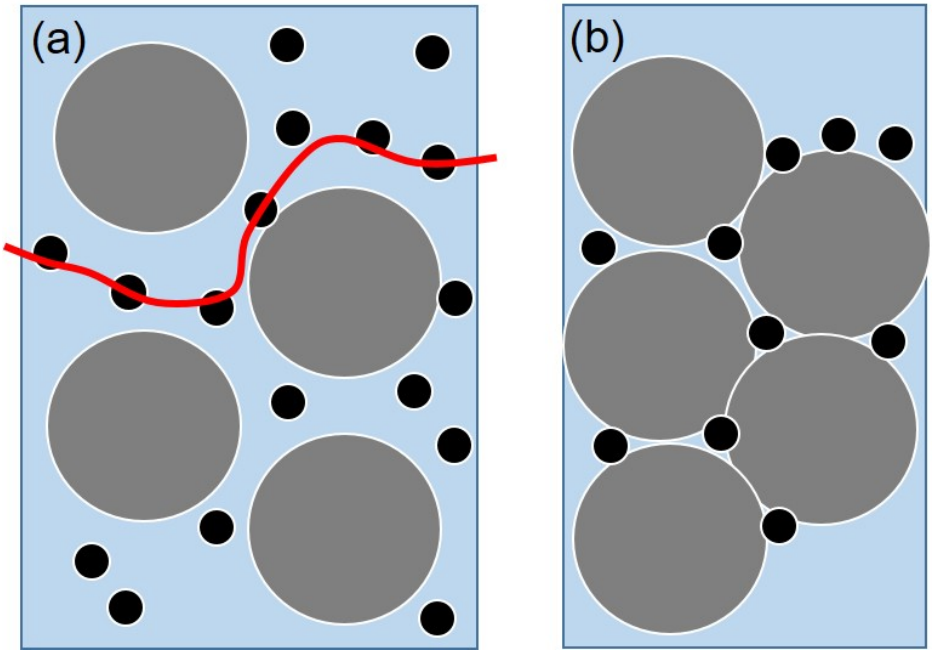

Figure 16. Illustration of microstructure in ternary PDMS hybrids. OA-ZnO nanoparticles are indicated in black. Secondary particle species (indicated in gray) provides a template for the formation of thermal conduction paths and can be chosen depending on the desired property profile (e.g. SiO_2 or PDMS).

In preliminary tests with silica particles as large particle filler species, a thermal conductivity of k = 0.64 +/- 0.03 $Wm^{-1}K^{-1}$ could be demonstrated in films of 1 mm thickness that retained an optical transparency of 0.72 at a wavelength of 450 nm.

In total 66 composite formulations were synthesized during the course of the program. The thermal conductivity of films with sufficient fracture resistance was evaluated using heat flow measurements. Heat-flow measurements on bulk films was performed at OSRAM Sylvania (Beverly, MA) in accordance with ASTM E1530 using a guarded heat flow meter. 0.85 mm thick films of PDSM and PDMS hybrids were prepared by film casting and subsequent curing. Calibration measurements were performed on OE-6630 – a commercial LED encapsulant that was provided by Dow Corning. The thermal conductivity of OE6630 was found to be k = 0.19 W/m*K with the uncertainty of 0.02 W/m*K which is consistent with information provided by Dow Corning. Table 2 summarizes the results of samples tested within the program.

Sample Number	Composition	Type	Thermal Conductivity
1	Pristine Al/PPMS(Dow Corning), 50wt%	Binary	0.32 W/m*K
2	VTMS modified Al nanoparticles/PPMS(Dow Corning), 50wt%	Binary	0.30 W/m*K
3	Commercial ZnO nanoparticles(d~18nm)/ PPMS(Dow Corning), 50wt%	Binary	0.45 W/m*K
4	Commercial ZnO nanoparticles(d~18nm)/ PPMS(50wt%)	Binary	0.46 W/m*K
5	PDMS capped ZnO/ PDMS, 15.5wt%	Binary	0.20 W/m*K.
6	PDMS capped ZnO/ PDMS, 30wt%	Binary	0.31 W/m*K.
7	PDMS capped ZnO/ PDMS, 40wt%	Binary	0.33 W/m*K.
8	OA-ZnO/PDMS, 46wt%	Binary	0.37 W/m*K.
9	OA-ZnO/PDMS, 41wt%	Binary	0.25 W/m*K.
10	OA-ZnO/PDMS, 54.8wt%	Binary	0.28 W/m*K.
11	OA-ZnO/PDMS, 56.5wt%	Binary	0.28 W/m*K.
12	OA-ZnO/PDMS, 60wt%	Binary	0.31 W/m*K.
13	OA-ZnO/PDMS, 58wt%	Binary	0.29 W/m*K
14	OA-ZnO/PDMS, φ_{ZnO}=3 wt%	Binary	0.34 W/m*K
15	OA-ZnO/SiO_2/PDMS, φ_{ZnO}=3 wt%	Ternary	0.39 W/m*K
16	OA-ZnO/SiO_2/PDMS, φ_{ZnO}=4 wt%	Ternary	0.51 W/m*K
17	OA-ZnO/SiO_2/PDMS, φ_{ZnO}=5 wt%	Ternary	0.64 W/m*K

3.3 Processing of PDMS hybrid encapsulants

The objective of this work effort was to understand the effect of particle addition on the mechanical properties of PDMS hybrids and to establish processing schemes for the fabrication of planar film and hemispherical lens shapes. The latter were chosen as representative form factors that are relevant in pc-LED designs.

Mechanical properties of PDMS hybrid films were determined using dynamic mechanical analysis (DMA). Particular emphasis was on the evaluation of the fracture toughness of film samples. The latter describes the resistance of films to fracture and is seen as a critical quantity in predicting the resistance of encapsulants to fracture due to thermal expansion during LED operation. Although the varying sample geometries did not allow for a quantitative determination of the fracture toughness of films, the measurements did reveal unambiguous qualitative trends. In particular, fracture toughness was found to decrease with increasing particle filling fraction. At inorganic content $f > 0.1$ PDMS/ZnO-OA hybrids were found to be susceptible to fracture during photothermal stability evaluation. No final assessment could be made regarding the cause for embrittlement (since the determination of fracture mechanism would entail a systematic analysis that was out of the scope of the present study). Systematic analysis of the effect of catalyst content revealed that embrittlement is at least in part caused by the interference of amine ligands with the platinum catalyst (Karstedt catalyst) used to initiate the crosslink reaction. Thus, in binary composites there is an optimum particle filling fraction that is determined by the balance of thermal conductivity (increases with particle filling fraction) and fracture toughness

(decreases with particle filling fraction). The competition of effects precludes the synthesis of high thermal conductivity encapsulants in the basis of binary composite systems and was the motivation for the development of the 'ternary hybrid approach'.

3.3.1 Measurement of Mechanical Properties using Dynamic Mechanical Analysis

Dynamic mechanical analysis was performed to better understand the role of particle addition on the mechanical properties of siloxane films and to evaluate the crosslink density of cured siloxane materials. DMA testing was performed using a TA-RSAG2, dynamical mechanical analyzer that is shown in Figure 17.

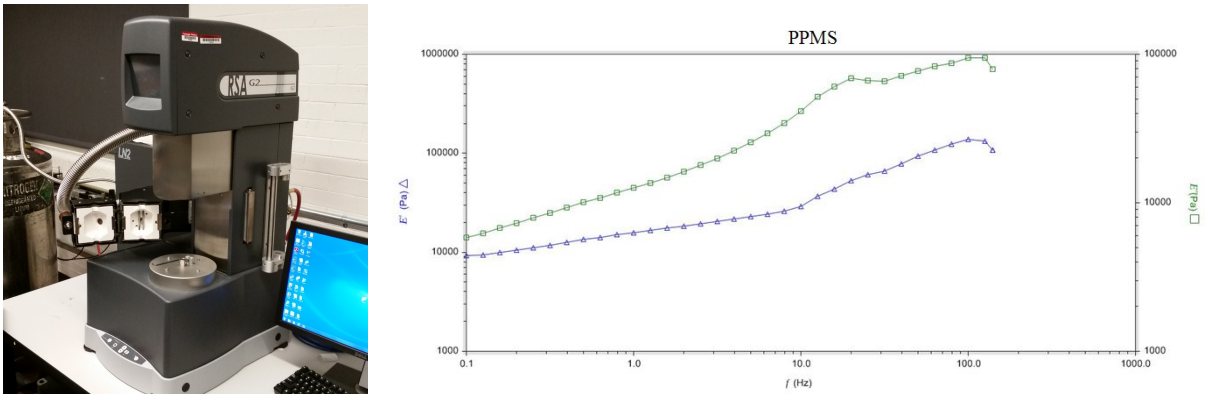

Figure 17. Picture on left: Picture of dynamic mechanical analyzer TA-RSAG2 as well as representative result for OE-6630/ZnO-OA (f = 0.15). Right: Compression tensile test performed in oscillatory mode over frequency range v = 0.1 Hz to 1 kHz. The dominance of the loss modulus (E'') indicates viscous liquid like response rather than solid like behavior.

Experiments were performed in compression mode, the geometry is a disc roughly 22mm in diameter and 1-2mm in thickness). The test consists of cycling through a range of frequencies from 0.1Hz to 140Hz at a strain of 1% in room temperature. Figure 17 also depicts representative results for a ZnO/OE6630 composite (volume filling fraction f = 0.15). The figure shows the dependence of the real (storage modulus, E') and imaginary (loss modulus, E'') modulus on the frequency of deformation. Note that in case of OE6630/ZnO-OA DMA reveals that the value of the loss modulus exceeds the respective value of the storage modulus at all tested frequencies. This demonstrates *liquid-like behavior* of the film. The liquid-like response is rationalized as a consequence of incomplete crosslinking that is caused by the interference of the amino functionality with an unknown additive in OE-6630. The challenge of incomplete crosslinking could be resolved by use of Gelest siloxane materials. The latter are considered 'research grade' and do not exhibit additives. Figure 18 depicts the typical result of a tensile stress strain test performed by DMA on Gelest-based PDMS hybrids.

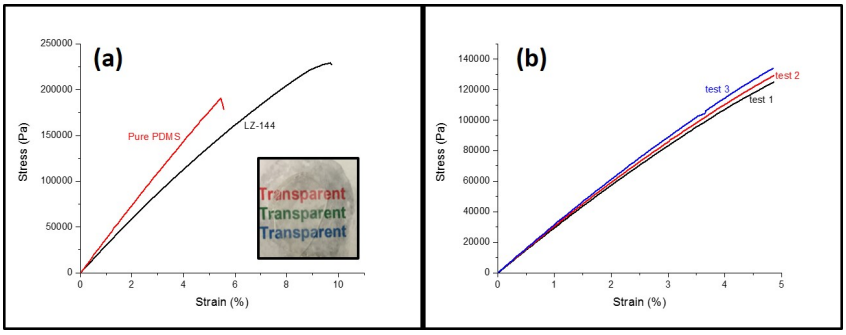

Figure 18. Plots of Strain and Stress curve obtained from tensile test a) Pure PDMS matrix (red) and PDMS/ZnO-OA hybrids (LZ-118); b) Hysteresis test. Inset: The photograph of OA capped ZnO in PDMS matrix with 50wt% ZnO used in tensile test.

DMA analysis was applied throughout the duration of the project to gauge the effectiveness of crosslink reactions and to evaluate the effect of particle addition on the mechanical properties of PDMS hybrids.

3.3.2 Processing of PDMS hybrids

The aim of this effort was to establish fabrication methodologies and conditions to enable the efficient sample preparation from hybrid encapsulants. Because of the difficulties in providing PDMS/alumina and PDMS/ZnO hybrid materials with sufficient mechanical robustness to allow for melt processing this effort focused on commercial hybrid encapsulants instead. Because the mechanical properties of particle filled resins depend on particle size and polymer/particle interactions (the latter being determined by the surface modification of particles) it is expected that the process parameters will translate to other PDMS hybrids compositions if suitable degree of dispersion can be accomplished. Three different heat-curable resins were evaluated during this study: pristine LED siloxanes (OE-6630) as well as siloxane/nanosilica hybrid resins (LC-9065, MS-1003) that were provided by Dow Corning. The hybrid siloxanes were chosen as 'model systems' as they are expected to mimic the expected rheological properties of particle-filled resins. The physical properties of these materials listed in Table 3.

Table 3. Physical Properties of the two-part resins received from Dow Corning®.

Physical Properties	Dow Corning® **LC-9065**	Dow Corning® **MS-1003**	Dow Corning® **OE-6630**
Mixing ratio (weight)	1:1	1:1	1:4
Viscosity (Pa-sec)	100	42.3	2.2
Hardness	Shore A - 36	Shore A - 52	Shore D - 43
Tensile Strength (MPa)	4.8	5.5	4.1
Working Time at @ 150^0C	5 min	1	2
Working Time at @ 25^0C	16 hour	48 hour	8 hour

As listed in Table 3, LC-9065, MS-1003, and OE-6630 are heat-curable, two-part, 1 to 1, 1 to 1, and 1 to 4 weight ratio resins, respectively. OE-6630 is a commercial LED siloxane encapsulant and have been used for the LED packages in the market. LC-9065 and MS-1003 are particle

filled siloxanes that are expected to exhibit similar mechanical and rheological properties to our novel particle systems. Specifically, hardness, elastic modulus, and viscosity of these materials are expected to resemble those of our novel particle systems since the processability depends highly on these physical properties. Ideally, the fabrication techniques developed and the fundamental understanding gained for these model materials would be applied to our novel particle systems.

The fabrication process that was developed combines mechanical micromilling with a three-step molding approach, including vacuuming the polymer mixtures to remove the air bubbles, centrifuging to fill the molds with the polymer mixtures, and thermal aging to cure the siloxane intermediates. Mechanical micromilling was used to create precise molds to facilitate our molding studies. Using this fabrication approach, we conducted during an Analysis of Variance study to determine conditions that allowed us to reliably fabricate lens shaped specimen of hybrid encapsulant materials. A micromolding process was developed (involving in progression, vacuum degassing, spin-casting, and thermal curing) to fabricate lens-shape features with varying diameter (4 mm and 7 mm) and depths/heights (1 mm and 1.5 mm). The lens features were fabricated directly on Golden Dragon LED packages. Qualitative and quantitative assessment of the fabricated lens-shape geometries was performed by high resolution imaging and optical three-dimensional (3D) surface/form characterization on metal molds and lens shapes, respectively. Furthermore, the surface quality of the fabricated pc-LED relevant geometries was assessed using white-light interferometry. The surface roughness and form error measurements were used as the performance metrics to evaluate the overall performance of the process as well as to assess its reproducibility. A DOE study was completed to identify the relevant parameters that determine sample fidelity; sample viscosity and spin conditions were determined to be critical parameters determining the quality of shapes. For all samples the required fidelity of shape parameters could be achieved – sample roughness was found to be about 200 nm, well in agreement with specifications provided by OSRAM Sylvania. Figure 18 summarizes the results (averaged over five specimen each).

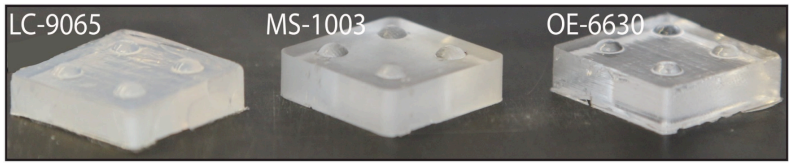

	4 mm diameter			7 mm diameter		
	Depth (mm)	Diameter (mm)	Surface Roughness (nm)	Depth (mm)	Diameter (mm)	Surface Roughness (nm)
Mold	1.011±0.009	4.021±0.012	218±23	1.512±0.011	7.031±0.019	254±32
Dow Corning® **LC-9065**	1.021±0.012	4.009±0.018	220±12	1.521±0.013	7.022±0.032	251±38
Dow Corning® **MS-1003**	1.014±0.011	4.017±0.016	216±13	1.509±0.013	7.016±0.024	239±34
Dow Corning® **OE-6630**	1.011±0.014	4.022±0.013	210±21	1.512±0.014	7.026±0.016	249±41

Figure 18. Representative images of 7 mm specimen of pristine and hybrid siloxane model systems along with respective variation of shape characteristics (averaged over five samples each).

Having the aforementioned successful molding results with the model particle systems using our robust fabrication technique, we also created two other LED relevant geometries, flat sheet-design and hemisphere dome-design (*5 mm* diameter) on one of the state-of-the-art LED packages (Golden Dragon) received from OSRAM SYLAVINA. Figure 19 shows the digital camera images of the flat sheet-design and hemisphere design with 5 mm diameter from three-different model materials. It should be noted that in Figure 19, different dyes were used to indicate different materials and clearly show the sheet-design when the cavities on Golden Dragon LED packages are filled. It was qualitatively observed from Figure 19 that our micromilling/micromolding based fabrication approach is capable of integrating our novel materials into Golden Dragon packages with two pc-LED relevant geometries from a variety of siloxane-intermediates/particle-dispersions.

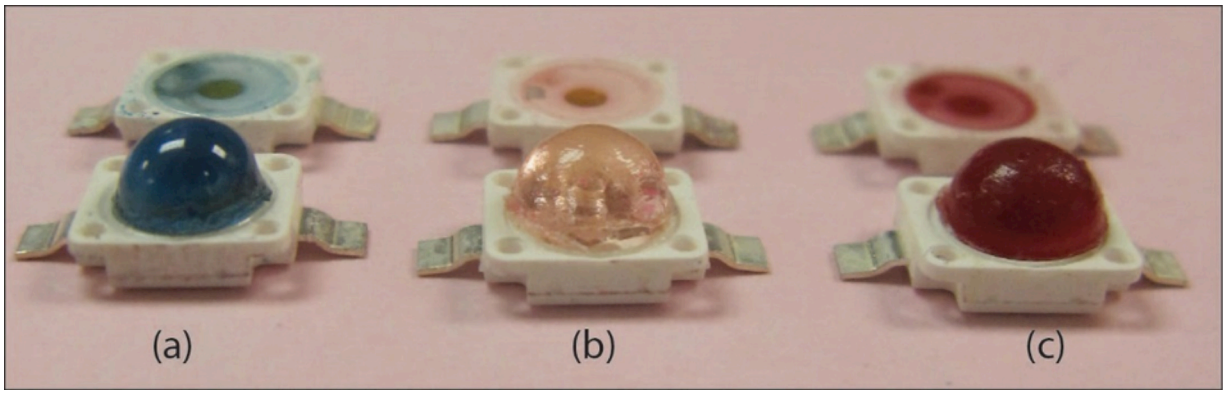

Figure 19. Demonstration of the capabilities of the fabrication approach for integration of PDMS hybrid materials into current LED packages with pc-LED relevant features from three-different materials possessing the physical properties resembling those of our novel hybrid systems. **(a)** LC-9065, **(b)** MS-1003, and **(c)** OE-6630.

It is worth noting that the flat sheet-design with OE-6630 (commercial LED encapsulant) is the state-of-the-art for pc-LED based solid state lighting and has been used with or without transparent lens attached to the current LED packages. From the processing standpoint, it is relatively easier to micromold OE-6630 into flat sheet-design features since OE-6630 is a low viscosity material. Indeed, it is possible to uniformly fill the cavities on the LED packages with OE-6630 using just the gravitational force for creating flat sheet-design features. However, other particle filled model siloxane encapsulants entail advanced manufacturing techniques to uniformly fill the cavities on the LED packages for accurately and reproducibly creating flat sheet-design features because of their different mechanical and rheological properties, such as viscosity, hardness, and elastic modulus. On the other hand, hemisphere dome-shape design features considered in this work could potentially enhance the optical performance of the current LED technology significantly but has not been utilized because of overheating problems due to low thermal conductivity of the existing LED encapsulants. However, it becomes rather challenging to accurately and reproducibly create these hemisphere dome-shape design features with high-viscosity materials since the existing fabrication methods are not plausible towards this end. As such, our micromilling/three-step micromolding approach addresses the shortcomings of the existing methods and provides an effective means for accurate and reproducible fabrication of flat sheet-design and hemisphere dome-design features on LED packages.

3.4 Modeling the Optical Transmittance of PDMS Hybrids

The objective of this research effort was to develop predictive models to evaluate of the optical properties (scattering cross section) of nanoparticle-filled siloxane encapsulants as well as siloxane/nanoparticle/template ternary blend systems with the goal to identify material compositions that minimize scattering losses induced by nanoparticle addition to the siloxane encapsulant. Three models - differing in complexity and computational cost – have been developed to evaluate the trade-off in balancing versatility and accuracy of optical models. Specifically, effective medium models (based on Maxwell Garnett and Bruggeman theories) were applied to predict compositions of core-shell particles that minimize optical scattering within a PPMS matrix. A core-shell Mie model was developed to validate effective medium predictions and to determine the optical properties of (individual) polymer-tethered nanoparticle systems embedded in PPMS. The model was applied to determine that minimum scattering of PMMA-modified alumina in PPMS is expected at a composition of approximately 56 vol% – in good agreement with effective medium predictions ($\phi_{inorg} \sim 48$ vol%). A finite difference time domain (FDTD) model was developed to evaluate the role of multiple scattering in densely particle filled encapsulants and to validate the predictions of the core-shell Mie model. In the following, the details of the Core-Shell Mie model will briefly be discussed.

Core Shell Mie Model

The scattering cross-section of ligand-tethered particles embedded in PDMS was calculated using core-shell Mie theory assuming constant mass density of the polymer shell and bulk optical properties. Calculations were performed using MATLAB. Specifically, the scattering cross section was calculated as

$$C^{\text{sca}} = \frac{2\pi}{k}\sum_{n=0}^{\infty}(2n+1)(|a_n|^2 + |b_n|^2) \quad (1)$$

where the sum was truncated when multipole contributions contributed less than 0.1% to the final result. In eq 1 a_n and b_n denote the Mie scattering coefficients for concentric core-shell systems that are defined as

$$a_n = \frac{\psi_n(y)[\psi_n'(m_2y) - A_n\chi_n'(m_2y)] - m_2\psi_n'(y)[\psi_n(m_2y) - A_n\chi_n(m_2y)]}{\xi_n(y)[\psi_n'(m_2y) - A_n\chi_n'(m_2y)] - m_2\xi_n'(y)[\psi_n(m_2y) - A_n\chi_n(m_2y)]}$$

$$b_n = \frac{m_2\psi_n(y)[\psi_n'(m_2y) - B_n\chi_n'(m_2y)] - \psi_n'(y)[\psi_n(m_2y) - B_n\chi_n(m_2y)]}{m_2\xi_n(y)[\psi_n'(m_2y) - B_n\chi_n'(m_2y)] - \xi_n'(y)[\psi_n(m_2y) - B_n\chi_n(m_2y)]}$$

with

$$A_n = \frac{m_2\psi_n(m_2x)\psi_n'(m_1x) - m_1\psi_n'(m_2x)\psi_n(m_1x)}{m_2\chi_n(m_2x)\psi_n'(m_1x) - m_1\chi_n'(m_2x)\psi_n(m_1x)}$$

$$B_n = \frac{m_2\psi_n(m_1x)\psi_n'(m_2x) - m_1\psi_n(m_2x)\psi_n'(m_1x)}{m_2\chi_n'(m_2x)\psi_n(m_1x) - m_1\psi_n'(m_1x)\chi_n(m_2x)}$$

Here, m_1 and m_2 are the refractive index of core and shell relative to the embedding medium, i.e. $m_i = n_i/n_m$; $x = kR_0$, and $y = kb$ are size parameters (with R_0 denoting the core radius and b the overall radius of the core-shell particle calculated based on the assumption of uniform density), and $k = 2\pi n_m/\lambda$ denoting the modulus of the wave vector at wavelength λ; n_m denotes the refractive index of the matrix. $\psi_n(z)$ and $\xi_n(z)$ are the Ricatti-Bessel functions (of order n) that are defined in terms of the spherical Bessel functions $j_n(z)$ and $y_n(z)$ as $\psi_n(z) = zj_n(z)$, $\chi_n(z) = zy_n(z)$ and $\xi_n(z) = zh_n(z)$ where $h_n(z) = j_n(z) + iy_n(z)$ denotes the spherical Hankel function of order n. Where appropriate the 'prime' sign indicates derivatives. Figure 18 depicts an exemplary result for the calculated scattering cross section of a PMMA Alumina particle embedded in poly(phenyl methyl siloxane) (PPMS) which form the basis for commercial LED encapsulants. The calculation was performed by making the following assumptions of the material parameters: d = 30 nm, $n_{c/Al2O3}$ = 1.8, $n_{s/PMMA}$ = 1.49, $n_{m/PPMS}$ = 1.55, $\varrho_{c/Al2O3}$= 3.95 g/cm^3, $\varrho_{s/PMMA}$= 1.188 g/cm^3, $\varrho_{m/PSAN}$= 1.08 g/cm^3.

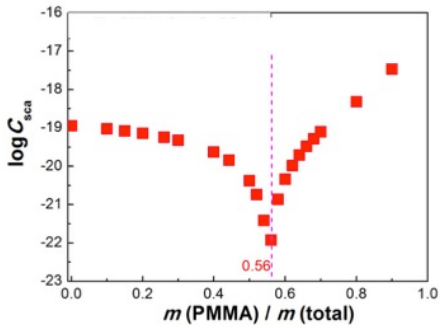

Figure 20. Scattering cross section of PMMA-tethered alumina particles embedded in PPMS matrix calculated using core-shell Mie Model. A polymer content of 0.56 (by weight) is expected to reduce the scattering cross section by a factor of 10^4.

Figure 20 reveals that the scattering cross section of particle fillers is highly sensitive to the shell composition of ligand layers. For example, at the specific composition of 56 wt% content of PMMA the scattering cross section of PMMA-tethered alumina particles embedded in PPMS is expected to be reduced by a factor of 10^4 as compared to the pristine particle analogs. The predictions of the core-shell Mie model were validated using finite element simulations as well as experimental reference systems that enabled the fabrication of suitable compositions (PSAN tethered silica in PMMA). Unfortunately, for the specific case of Alumina-PMMA suitable compositions could not be accomplished. However, core-shell Mie simulation motivated the use of octylamine ligands in PDMS/ZnO-OA hybrid materials. OA ligands are expected to reduce the scattering cross section by approximately 50% as compared to the pristine particle fillers.

3.5 Photothermal Stability Testing of PDMS Hybrid Encapsulants

Photothermal stability is a key characteristic to ascertain the suitability of a hybrid siloxane for LED application. This is because even small (scattering or absorption) losses result in the rapid heat accumulation and degradation of materials. A photothermal stability testing device was designed and constructed to evaluate the stability of samples at high flux levels of blue LED light

and elevated temperatures (T = 150 deg C). The test evaluates the transmittance of materials during the irradiation power at 450 nm up to 22 W/cm^2 and temperatures up to 160 ºC. The degradation time is defined as the duration for loss in transmittance by 20%. Note that the test conditions represent a higher 'stress' on sample materials as is actually encountered in LED designs (the flux experienced by the silicone cast on the LED chip at 350 mA is only 0.5 W/mm^2). These 'accelerated degradation' conditions were chosen because they were found to represent a more reliable measure for the long-term operational stability of materials.

A challenge associated with this test has been the mechanical stresses that the material experiences when mounted in the testing setup. For example, for most materials, premature failure through mechanical cracking was observed rather than light-induced coloration of the material. It was shown that for films to be 'mechanically stable' during photothermal stability testing, mechanical properties have to fall within defined ranges such as moduli E ~ 5 MPa and large strain-to-fracture (~ 20%). Since these properties require the tuning of molecular characteristics (i.e. crosslink density) as a function of particle loading levels, optimum compositions have to be determined for each loading level. At present, we have optimized the composition for testing of hybrid films with ~ 50 wt% inorganic loading (we are currently working on films with >70 wt% loading levels). For these films our results indicate *excellent photothermal stability characteristics*. In the longest duration test (205 hours) the sample eventually fractured due to mechanical impact – no photo-induced damage was discernible. We are thus still in the process of quantifying the ultimate lifetime of our materials. We note that the test is designed to provide a conservative estimate for material stability. This is because the conditions reflect the upper limit of expected temperature in an LED device (i.e. the total sample temperature corresponds to the 'limiting temperature' that is only expected in the vicinity of phosphor particles in actual dc-LEDs)

Figure 21 displays a typical result obtained from photothermal stability test. For this test a circular planar PDMS/ZnO-OA hybrid film (cross sectional area 1 in^2, filling fraction f ~ 40 wt%) was mounted in the testing device. Light intensity is 34 W/cm2, sample holder T=150 °C, sample thickness was 1 mm. Initial rise in transmission is due to heating up of the photodetector.

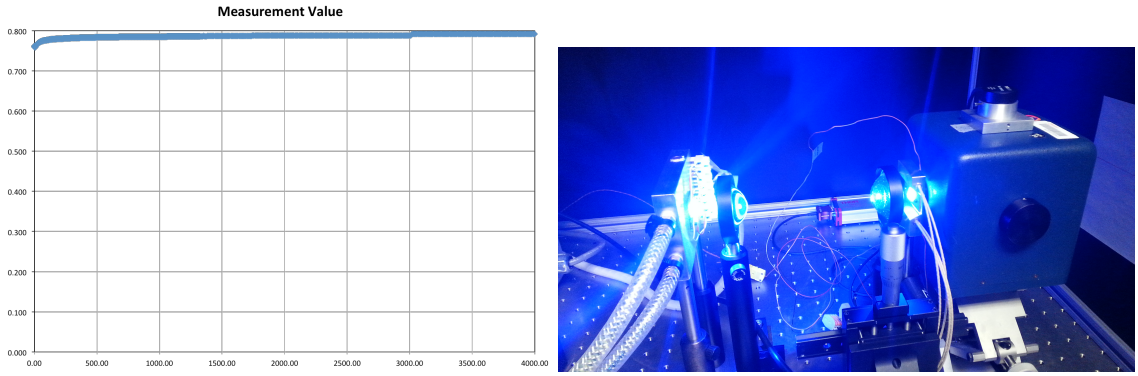

Figure 21. Transmission *vs* time plot for photothermal stability test of PDMS/ZnO-OA (20 wt%, LZ 58, time in 'seconds'). No degradation is observed after 4000 seconds of testing. Image on right shows image of testing process. The highest blue flux is 22 W/cm^2 (0.22 W/mm^2). A second tester has been built with improved optics. Expected blue light flux is up to 30 W/cm^2 (0.3 W/mm^2). For comparison, the flux experienced by the silicone cast on the LED chip at 350 mA is 0.5 W/mm^2.

It is noted that PSAN-based materials displayed visible degradation under the current test

conditions after only 1-2 minutes (PMMA materials were found to remain stable for about 5 minutes). In contrast, the stability of ZnO-OA based hybrid materials presents a dramatic improvement and is encouraging with respect to LED applications.

IV. Products

4.1 Impact on Human Resource Development

The funding received under award #DE-EE0006702 supported the work of seven graduate students and one postdoctoral researcher.

Dr. Amir Khabibullin, currently employed as postdoctoral researcher at Chemistry Department, University of Toronto, Canada

Clare Mahoney, PhD 2015, currently employed as NRC Fellow at the Air Force Research Laboratory, Dayton, OH

Shubhaditya Majumdar, PhD 2015, currently postdoctoral fellow at the Department of Chemical Engineering, University of California, Santa Barbara, CA

Emrullah Korkmaz, PhD 2017, currently postdoctoral fellow at the Department of Mechanical Engineering, Carnegie Mellon University, PA

Jiajun Yan, Chemistry Department, Carnegie Mellon University, PhD expected in 2018

Zongyu Wang, Chemistry Department, Carnegie Mellon University, PhD expected in 2019

Jaejun Lee, Department of Materials Science and Engineering, PhD expected in 2019

Zhao Lu, Department of Materials Science and Engineering , PhD expected 2020

4.2 Publications

In total 15 manuscripts were published in peer reviewed research journals (see references 1-15 below). Furthermore 12 invited presentations were given that reported on the results obtained as part of the project (not shown here).

[1] Dang, A.; Hui, C. M.; Matyjaszewski, K.; Bockstaller, M. R. Design and fabrication strategies for high transparency polymer nanocomposites with dynamic tunable optical response. *SPIE Organic Photonics+ Electronics*, 91810U-91810U-6, 2014.

[2] Schneider, D.; Schmitt, M.; Hui, C. M.; Sainidou, R.; Rembert, P.; Matyjaszewski, K.; Bockstaller, M. R; Fytas, G. Role of Polymer Graft Architecture on the Acoustic Eigenmode Formation in Densely Polymer-Tethered Colloidal Particles. *ACS Macro Letters*, 3, 1059-1063, 2014.

[3] Dang, A.; Ojha, S.; Hui, C. M.; Mahoney, C.; Matyjaszewski, K.; Bockstaller, M. R. High-Transparency Polymer Nanocomposites Enabled by Polymer-Graft Modification of Particle Fillers. *Langmuir*, 30, 14434-14442, 2014.

[4] Grabowski, C. A.; Koerner, H.; Meth, J. S.; Dang, A.; Hui, C. M.; Matyjaszewski, K.; Bockstaller, M. R.; Durstock, M. F.; Vaia, R. A. Performance of dielectric nanocomposites: Matrix-free, hairy nanoparticle assemblies and amorphous polymer–nanoparticle blends. *ACS Appl. Mater, & Interfaces* 6, 21500-21509, 2014.

[5] Alonso-Redondo, E.; Schmitt, M.; Urbach, Z.; Hui, C. M.; Sainidou, R.; Rembert, P.; Matyjaszewski, K.; Bockstaller, M. R.; Fytas G. *Nature Commun.*, 6, 2015.

[6] Bockstaller, M. R. Progress in polymer hybrid materials. *Progress in Polymer Science*, 40, 1-2, 2015.

[7] M. Schmitt, J. Choi, C. M. Hui, B. Chen, E. Korkmaz, J. Yan, S. Margel, O. B. Ozdoganlar, K. Matyjaszewski, M. R. Bockstaller "Processing Fragile Matter: Effect of Polymer Graft Modification on the Mechanical Properties and Processibility of (Nano)Particulate Solids" *Soft Matter*, 2016, **12**, 3527.

[8] Yan, J.; Pan, X.; Schmitt, M.; Wang, Z.; Bockstaller, M. R.; Matyjaszewski, K. Enhancing initiation efficiency in metal-free surface-initiated atom transfer radical polymerization (SI-ATRP). *ACS Macro Letters* 5, 661-665, 2016.

[9] Khabibullin, A.; Bhangaonkar, K.; Mahoney, C.; Lu, Z.; Schmitt, M.; Sekizkardes, A. K.; Bockstaller, M. R.; Matyjaszewski K. Grafting PMMA Brushes from α-Alumina Nanoparticles via SI-ATRP. *ACS Appl. Mater. & Interfaces*, 8, 5458-5465, 2016.

[10] Włodarczyk, B.; Ferebee, R.; Bockstaller, M. R.; Pietrasik J. Synthesis of hydroxyapatite particles with in situ immobilized ATRP initiator. *Polymer* 72, 348-355, 2015.

[11] Ding, H.; Yan, J.; Wang, Z.; Xie, G.; Mahoney, C.; Ferebee, R.; Zhong, M.; Daniel, W.F.M.; Pietrasik, J.; Sheiko, S. S.; Bettinger, C. J.; Bockstaller, M. R.; Matyjaszewski K. *Polymer*, 107, 492-502, 2016.

[12] Koerner, H.; Opsitnick, E.; Grabowski, C.A.; Drummy, L. F.; Hsiao, M.-S.; Che, J.; Pike, M.; Person, V.; Bockstaller, M. R.; Meth, J. S.; Vaia, R. A. Physical aging and glass transition of hairy nanoparticle assemblies. *J. Polym. Sci. Part B: Polym. Phys.* 54, 319-330, 2016.

[13] Wang, Z.; Mahoney, C.; Yan, J.; Lu, Z.; Ferebee, R.; Luo, D.; Bockstaller, M. R.; Matyjaszewski, K. Preparation of Well-Defined Poly(styrene-co-acrylonitrile)/ZnO Hybrid Nanoparticles by an Efficient Ligand Exchange Strategy. *Langmuir*, 32, 13207–13213, 2016.

[14] Mahoney, C.; Hui, C. M.; Majumdar, S.; Wang, Z.; Malen, J. A.; Tchoul, M. N.; Matyjaszewski, K.; Bockstaller, M. R.Enhancing thermal transport in nanocomposites by polymer-graft modification of particle fillers. *Polymer* 93, 72-77, 2016.

[15] Schmitt, M.; Zhang, J.; Lee, J.; Lee, B.; Ning, X.; Zhang, R.; Karim, A.; Davis, R. F.; Matyjaszewski, K.; Bockstaller, M. R. *Science Advances*, 2, e1601484, 2016.

4.3 Patents

One patent application was filed based on research performed within the project funded by DE-EE0006702.

COMPOSITE COMPOSITIONS AND MODIFICATION OF INORGANIC PARTICLES FOR USE IN COMPOSITE COMPOSITIONS, International Patent Application, Application Number: PCT/US17/14723. Filing Date: 24-Jan-2017.